

## **A SKELETAL REFERENCE DOSIMETRY MODEL FOR THE ADULT FEMALE**

**Kayla N. Kielar and Wesley E Bolch**

University of Florida  
Department of Nuclear and Radiological Engineering  
University of Florida, Gainesville, FL 32611  
kay21@ufl.edu; wbolch@ufl.edu

**Amish P. Shah**

Department of Radiation Oncology  
MD Anderson, Orlando, FL 32806  
amish@ufl.edu

### **ABSTRACT**

Absorbed dose estimates to the skeletal tissues (active bone marrow and endosteum) are an essential feature of risk estimates in both occupational and medical dosimetry. At present, the vast majority of skeletal reference models (SRMs) used for these purposes are based on studies in the late 1960s and early 1970s at the University of Leeds in which a novel optical scanning method was used to obtain linear chord-length distributions across several skeletal sites of a single 44-year male subject. These data form an essential component of the ICRP's SRM published in ICRP Publications 30, 70, and 89. Recently, researchers at the University of Florida's Bone Imaging & Dosimetry Project have developed an image-based skeletal reference model for the adult male at an age representative of cancer patients undergoing radionuclide therapy (66-year). In the present study, initial work on an adult male cancer patient was further developed to add a companion SRM, the adult female cancer patient. A 64-year-old female cadaver was selected having a body-mass index of 23.8 kg m<sup>-3</sup> and a cause of death presenting a low probability of skeletal deterioration. In-vivo CT images were acquired prior to bone harvesting at 13 skeletal sites, all with high percentages of active bone marrow. Next, high-resolution ex-vivo CT images were acquired from which volumes of both cortical bone and trabecular spongiosa were determined via image segmentation. Finally, physical sections of spongiosa were cut and imaged via microCT. An entire skeletal mass database was established for a female reference dosimetry model, including percentages of active marrow for those bone sites that contain active marrow. Both sets of images (ex-vivo CT and ex-vivo microCT) will be combined under Paired-Image Radiation Transport (PIRT) via methods described previously by Shah et al. (JNM 46:344-353; 2005). Once fully established, skeletal dose estimates from the UF reference female skeletal model may be scaled to individual patients via CT-based measurements of spongiosa volume (adjustments at the macroscopic level) and potentially CT-based measurements of bone mineral density (adjustments at the microscopic level).

**KEYWORDS:** skeletal dosimetry; bone; marrow; skeletal masses

## 1. INTRODUCTION

In order to predict the risk of bone cancer, an accurate assessment of absorbed dose to skeletal tissues is necessary. Concerning these tissues, the limiting factor in radiation protection is the toxicity of hematopoietically active bone marrow. Bone marrow is made up of red active marrow which includes the hematopoietically active elements, and yellow inactive fatty marrow. Particular tissues of interest for cancer risks are the hematopoietic stem cells (leukemia) and osteoprogenitor cells (bone cancer) of the trabecular endosteum within the red active marrow.

Previous analysis has shown that absorbed dose is an accurate measure of hematological toxicity, but only if the absorbed dose estimate is specific to the particular patient. At present, the vast majority of skeletal reference models (SRMs) used for these purposes are based on studies in the late 1960s and early 1970s at the University of Leeds in which a novel optical scanning method was used to obtain linear chord-length distributions across several skeletal sites of a single 44-year male subject. These data form an essential component of the ICRP's SRM published in ICRP Publications 30, 70, and 89.

MIRD methodologies of absorbed dose,  $D = A \times S$ , requires separate knowledge of the cumulated activity within the source (marrow or bone), and the radionuclide S value (absorbed dose per unit cumulated activity). Much research has been done to assess the cumulated activity within the source, while little has been done to make patient-specific assessments of absorbed dose per unit cumulated activity. Furthermore, these dose calculations requires known reference values such as the fraction of energy deposited in a target tissue and the mass of those target tissues.

Recent work has been done at the University of Florida Bone Imaging and Dosimetry Group to more accurately determine the fractional energy deposition in bone for alpha emitters and beta emitters as a function of bone site. Also, complete sets of skeletal macrostructural and microstructural data, in a format sufficient for radiation transport simulations, have been established for an image-based skeletal reference model for the adult male at an age representative of cancer patients undergoing radionuclide therapy (66-year). Relevant tissues of the microstructure, such as the bone trabeculae, bone endosteum, and marrow cavities were accounted for through image-based techniques. Skeletal tissue masses, which are important in determining radionuclide S values, have been reported to update those summarized in ICRP Publications 70 and 89.

To provide an accurate dose assessment in radiation protection, the reference skeletal dosimetry model must be patient-specific. That is, it should be designed to match as closely as possible to the average or typical individual in the worker population. The skeletal tissue doses are then to be used only to establish dose limits based upon an acceptable risk or radiation induced effects (stochastic or non-stochastic). Previous work has been done to give mass estimated for the male model, however, work had not been done to assess differences based on gender. To date, there is no skeletal reference female model and this paper serves to present a companion skeletal reference model to the adult male.

## 2. BACKGROUND

Bone is constantly remodeled in order to maintain constant levels of  $\text{Ca}^{2+}$  and  $\text{PO}_4^{3-}$ , and as a result of mechanical stress the particular bone site endures. The functional portion of bone responsible for this remodeling are the osteoblasts, responsible for creating collagen to strengthen bone, osteocytes, responsible for controlling the mineral balance, and osteoclasts which destroy bone mineral tissue, shown in Fig 1. Osteoporosis is the most common bone disease in the United States and is a disorder which causes bone resorption to become much greater to bone formation. It seems that osteoclasts become more numerous, while the number of osteoblasts greatly declines. Thus, marrow cavities seem to get larger as trabeculae have unfilled cavities seen in Fig 2.

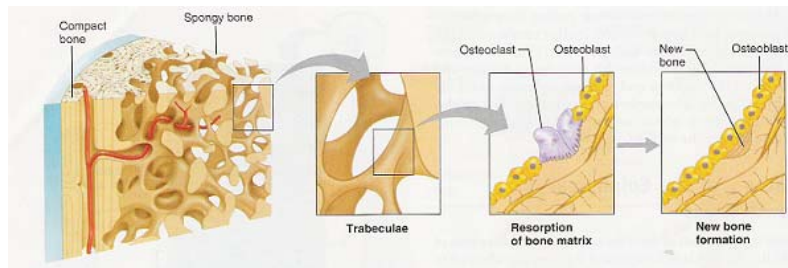


**Figure 1. Remodeling of spongy bone.**

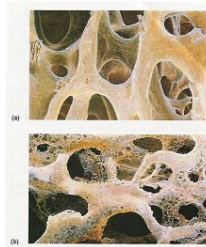


**Figure 2. The affects of osteoporosis on the spongiosa in a) normal bone, and b) osteoporetic bone.**

The mass of a skeletal site is strongly affected by Marrow Volume Fraction (MVF), or amount of marrow compared to the total skeletal mass. Osteoporosis changes the MVF, thus changing bone mass. Thus, for patient specific estimates of absorbed dose, marrow masses must be made as specific as possible and must include osteoporetic state. Currently, work is being done at the University of Florida to relate the measured BMD in a bone site of a patient to an estimate of the MVF of the bone site. It is hoped to build a dataset of reference individuals with varying microstructure that is scalable to a particular patient.

Radiation transport is done via the Paired Image Radiation Transport (PIRT) Code. This code is the way in which the user communicates with EGS by means of subroutines to provide geometry, define which features to use, and produce output. PIRT allows actual macrostructural (bone geometry) and microstructural (trabecular geometry) images to be read in and calculates the fraction of energy deposited in marrow cavities and other regions of bone (absorbed

fraction). This radiation transport method serves as the benchmark for all existing skeletal dosimetry calculations.

PIRT provides mean absorbed fraction data for several source target combinations along with 95% confidence intervals and relative errors. The possible sources of radiation emitters are Trabecular Active Marrow (TAM), Trabecular Inactive Marrow (TIM) or adipose tissue, Trabecular Bone Volume (TBV), Trabecular Bone Surface (TBS), and Cortical Bone Volume (CBV). The possible targets are the same, with the inclusion of the Shallow Active Marrow (TAMs) which is defined as 50 microns from the surface of any trabecular bone region. This serves as the endosteum target under current methodologies. The cellularity factor (CF) is varied and is the fraction of marrow that is active (1-fat fraction).

### **3. MATERIALS AND METHODS**

#### **3.1. Female Cadaver Selection**

A female cadaver was selected through the State of Florida Anatomical Board located on the UF campus. The cadaver was selected in order to represent an average, healthy female for use in medical dosimetry. Selection criteria included (1) an age between 50 -75 years, (2) a body-mass index between 18.5 – 25 kg m<sup>-2</sup> (CDC recommended healthy range), and (3) a cause of death presenting a low probability of skeletal deterioration. The subject selected was a 64 year old female, 63 inches tall and 135 pounds. The subject thus had a body-mass index of 23.83 kg m<sup>-3</sup> and died of respiratory complications. A bone densitometry measurement determined a t-score of 1.55, putting the subject 1.55 standard deviations below the mean for age 30. Therefore, the subject is in an osteoporetic bone state.

#### **3.2. Skeletal-Image Database**

Several imaging modalities and image processing techniques were required in order to provide a complete skeletal database for the reference female model. First, two whole body in-vivo images were acquired using a multi-slice helical CT at 1mm slice thickness. In order to capture the whole body, the top of the body was imaged first, then the bottom. These in-vivo images will be used to construct three dimensional anatomical models of those skeletal sites which could not be completely harvested (e.g. ribs, cranium).

A contoured in-vivo image of the cranium showing the separation of the left parietal, right parietal, occipital, frontal, facial bones, and other bones (sphenoid, ethmoid, temporal) are shown in Fig 3 and 4. Furthermore, the images will provide a basis for planning the harvest of skeletal sites. The images were reconstructed using a B80 bone filter at the best possible resolution to capture the entire body. The CT images were stored within the UF Department of Nuclear and Radiological Engineering for data storage and image processing.



**Figure 3. In-vivo contoured image of the cranium, showing the separation of the lobes: left parietal (orange), right parietal (yellow), occipital (green), facial bones (pink), cortical bone (blue) and other bones (red).**

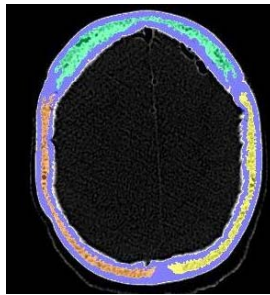


**Figure 4. In-vivo contoured image of the cranium showing the separated lobes: Left parietal (orange), right parietal (yellow), and frontal (green).**

Next, skeletal harvesting of those 13 skeletal sites containing the highest percentages of active marrow was performed. These included the cranial cap (parietal, occipital, and frontal lobes), clavicles (2), scapulae (2), entire vertebral column (cervical, lumbar, thoracic, and sacrum), ribs (3 from each side), os coxae, proximal humerii (2), proximal femora (2), mandible, and sternum. These sites were cleaned, labeled, bagged, and stored in a freezer until ex-vivo micro imaging could be performed.

High-resolution ex-vivo CT images were acquired from the harvested skeletal sites at 1.0 mm slice thickness, with the best possible in-plane resolution (limited by sample size). The field of view (FOV) ranged from about 5.0 cm for the ribs and 33.2 cm for the os coxae. These higher resolution CT images will be used to determine volumes of both cortical bone and trabecular spongiosa for each skeletal site through the program CT\_Contours based upon Interactive Data Language (IDL) version 6.0. Samples of the ex-vivo contoured images are shown for the femur in Fig 5. The separation of the femoral head and neck is shown. These images will also be used to determine the best location in that bone to extract a sample for micro imaging. Eventually, they will provide the 3D anatomic macrostructural model for paired-image radiation transport (PIRT) simulations.

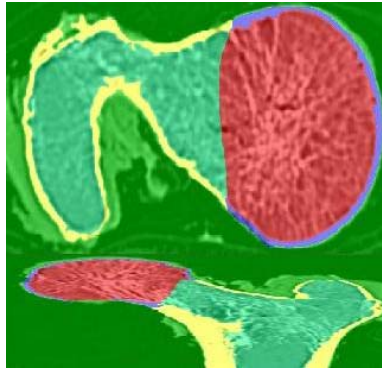


**Figure 5. Transverse (top) and Coronal (bottom) Contoured ex-vivo image of the femur, showing the separation of the femoral head and neck.**

After all ex-vivo CT images were acquired and volumes were determined, physical sections of marrow intact trabecular spongiosa were cut from each bone site and imaged via microCT. There were limitations on sample size due to bone shape, cost, and the microCT imaging system. Micro CT of the 35 cuboidal samples from the 13 major skeletal sites was performed on a desktop cone beam  $\mu$ CT80 scanner (Scanco Medical AG, Bassersdorf, Switzerland) at a 30 micron resolution. This resolution is relatively much higher than the previously 60 micron resolution used in the UF reference male skeletal database.

Post-acquisition image processing steps were then performed in order to determine marrow volume fraction (MVF), trabecular bone endosteum volume (TBE) fraction, and trabecular bone volume (TBV) fraction. These steps included (1) extraction of a region of interest (ROI) to remove trabecular bone from the image; (2) applying a median filter to improve the signal-to-noise ratio (SNR); (3) determining a threshold to best classify the voxels as either bone or marrow; and (4) segmentation of the ROI into a binary image based on the threshold gray-level value. The thresholding of trabecular spongiosa was performed using those techniques proposed by Didier et al. Here, visual inspection of the image gradient magnitude demonstrates the ability to retrieve sample volumes with a 1% accuracy at 30- $\mu$ m voxel resolution.

Once filtered and segmented, the volume fraction of the respective bone sites were used to report masses of red bone marrow (RBM), yellow (inactive) bone marrow (YBM), cortical bone volume (CBV), and total skeletal spongiosa mass. The term spongiosa describes all tissues interior to the CBV (e.g., TBV, TBE, RBM, and YBM together). More detailed definitions of skeletal tissues can be found in Appendix A. An entire skeletal mass database was established for a female reference dosimetry model, including percentages of active marrow for those bone sites that contain active marrow.

### **3.3. Mass Calculation**

Mass estimates require both the macrostructural volume information (contoured ex-vivo CT images), microstructural volume information (filtered and segmented microCT spongiosa images), and the volume percentage of hematopoietically active versus inactive bone marrow for each skeletal site (marrow cellularity). Marrow cellularity can vary anywhere from 10% to

100% (no adipose tissue). Therefore, this reference individual does not have one single value of total active marrow mass, but a range of potential masses dependent upon the marrow cellularity chosen. The reported masses use those cellularities provided by ICRP Publication 70, purely as a comparison purpose only. A detailed definition of mass calculations for every skeletal site is provided in Appendix A and B.

### 3.3.1 Bone sites containing active marrow

Masses were calculated for the 13 major bone sites containing active marrow. Densities for all skeletal regions were taken from ICRU 46 (1992). For those sites where multiple cuboidal samples were taken, the marrow volume fractions were volume averaged. The mass of red bone marrow (RBM) at skeletal site  $j$  was calculated as:

$$(m_{RBM})_j = (SV)_j (MVF)_j (CF)_j (\rho_{RBM})_j, \quad (1)$$

where  $SV_j$  is the spongiosa volume,  $MVF_j$  is the marrow volume fraction, and  $CF_j$  is the cellularity factor for skeletal site  $j$ , while  $\rho_{TAM}$  is the mass density of active marrow ( $1.03 \text{ g cm}^{-3}$ ).

The trabecular bone endosteum (TBE) and the trabecular bone volume (TBV) are calculated by:

$$(m_{TBE})_j = (SV)_j (EVF)_j \left[ (\rho_{TAM})_j (CF)_j \times ((\rho_{TIM})_j (1 - CF)_j) \right], \quad (2)$$

$$(m_{TBV})_j = (SV)_j (BVF)_j (\rho_{TBV})_j, \quad (3)$$

where  $EVF_j$  and  $BVF_j$  are the endosteal layer and bone trabeculae volume fractions at skeletal site  $j$ , respectively; while  $\rho_{TBE}$  and  $\rho_{TBF}$  are the mass densities of the endosteal layer and bone trabeculae layer:  $1.03 \text{ g cm}^{-3}$  and  $1.92 \text{ g cm}^{-3}$ , respectively. The endosteum layer is defined as all those tissues 50 microns away from all bone surfaces inside the cortical shell.

The mass of the inactive marrow (YBM) is calculated as:

$$(m_{YBM})_j = (SV)_j (MVF)_j (1 - CF)_j (\rho_{YBM})_j \quad (4)$$

where  $SV_j$  is the spongiosa volume,  $MVF_j$  is the marrow volume fraction, and  $CF_j$  is the cellularity factor for skeletal site  $j$ , while  $\rho_{TIM}$  is the mass density of inactive marrow ( $0.98 \text{ g cm}^{-3}$ ).

Through use of the ex-vivo CT image, cortical bone volume was determined by image segmentation. The mass of the cortical bone for skeletal site  $j$  can be determined as:

$$(m_{CBV})_j = (CBV)_j (\rho_{CBV})_j, \quad (5)$$

where  $CBV_j$  is the cortical bone volume ( $\text{cm}^3$ ), and  $\rho_{CBV}$  is the density of cortical bone ( $1.92 \text{ g cm}^{-3}$ ).

### 3.3.2 Bone sites not containing active marrow

Since marrow volume fractions were not available for the extremities, microstructural data was used from a similar bone site. The marrow volume fraction of the humerus was used for the

proximal and distal ends of the lower arm bones. For the lower leg bones, the marrow volume fraction of the femoral neck was used. Masses were calculated for the RBM, YBM, CBV, as in equations (3), (4), and (5) above. For the proximal and distal ends, the mass of the trabecular bone endosteum (TBE) was calculated as in equation (2).

Since there is no active marrow in the lower extremities, masses of the endosteum for the proximal and distal ends were calculated by:

$$(m_{TBE})_j = (SV)_j (EVF)_j (\rho_{TIM}) \quad (6)$$

where the definitions are as previously defined.

Since there is no bone trabeculae in the medullary cavities, masses of the endosteum were mathematically derived. The volume of the endosteum for skeletal site j was found by:

$$V_j = \pi \left[ (R_1)_j^2 - (R_2)_j^2 \right] L_j (\rho_{TIM}) \quad (7)$$

where  $R_1$  is the radius of the medullary cavity for skeletal site j,  $R_2$  is  $R_1 - 50$  microns, and  $L_j$  is the length of the medullary cavity for skeletal site j. The endosteum volume fraction (EVF) is then calculated as:

$$(EVF)_j = V_j / (SV)_{m,j} \quad (8)$$

where  $V_j$  is as defined above, and  $SV_{m,j}$  is the spongiosa volume of the medullary cavity in skeletal site j.

The mass is then calculated by:

$$(m_{TBE})_j = (SV)_j (EVF)_j (\rho_{TIM})_j \quad (9)$$

where the definitions are as previously defined. Again, more detailed definitions dependent on skeletal site is given in Appendix A.

### 3.4 Paired Image Radiation Transport

PIRT was executed for all possible source and target combinations at cellularities ranging from 10% to 100% for 13 bone sites for which macrostructural and microstructural image data was obtained and processed. These are the bone sites containing active marrow and are as follows: cranium, mandible, clavicles, scapulae, sternum, cervical vertebrae, thoracic vertebrae, lumbar vertebrae, sacrum, ossa coxae, proximal humeri, and proximal femora. Specific absorbed fractions were calculated for all bone sites and source target combinations. Three comparisons were made: 1. A comparison of each bone site and its corresponding source and target combinations (varying cellularity factor), 2. A comparison among variation of all bone sites (due to physical size and microstructural changes), and 3. A comparison of all sources (TAM, CBV, TIM, TBV, TBS) for each bone site.

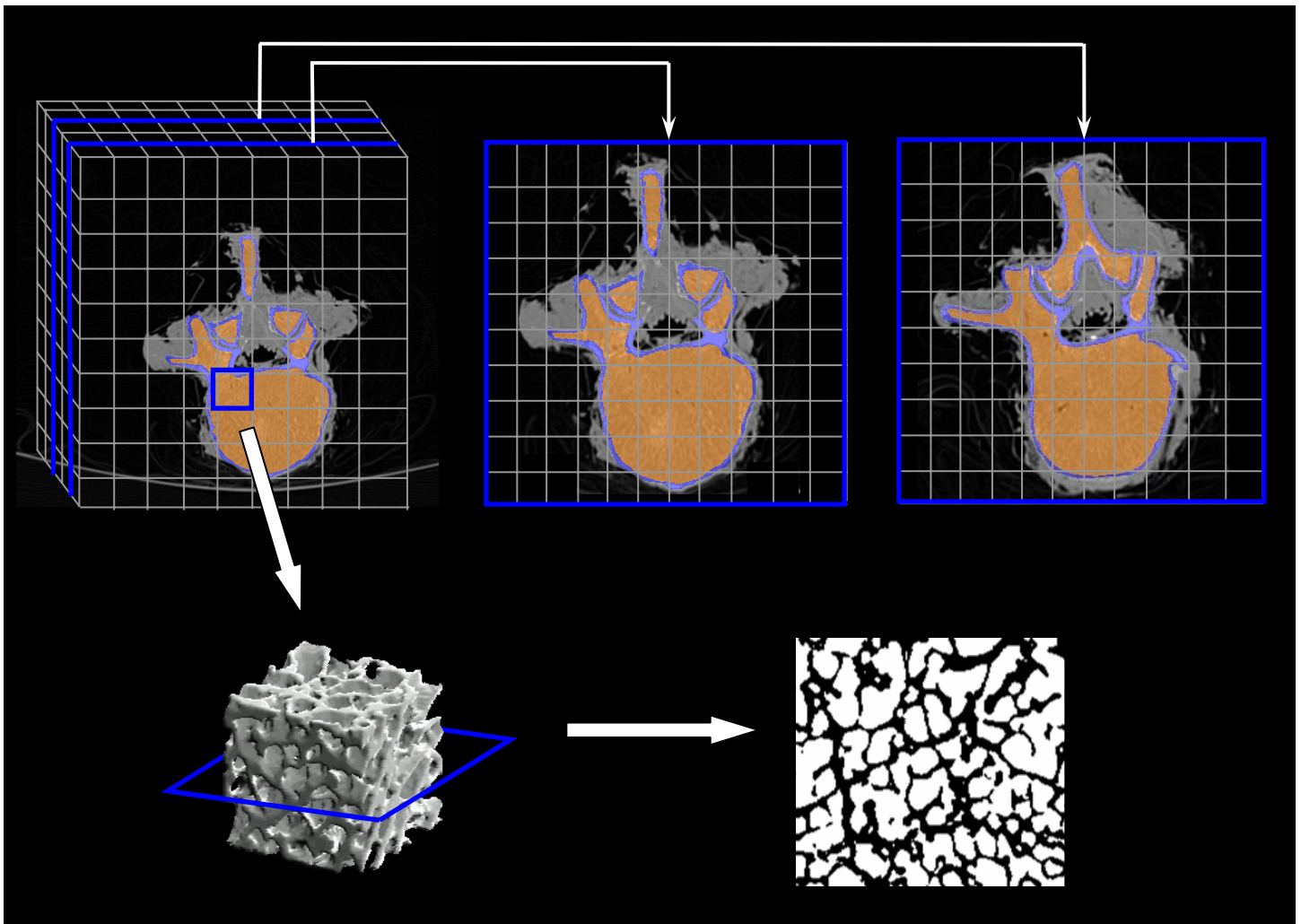


**Figure 6. Paired Image Radiation Transport.**

## **4. RESULTS AND DISCUSSION**

### **4.1 Spongiosa Volume and Percentages**

The spongiosa volume and percentage of total for reference female (RF) was first compared to a population of database of 20 cadavers, 10 male and 10 female, provided by Brindle et al. The spongiosa volumes were averaged by skeletal site for female cadavers, male cadavers, and then an average of all cadavers of either sex. Reference female seems to match well to the average female with respect to total spongiosa volume and percentages of total. The total spongiosa volume is remarkably close at less than 1% difference. RF has less spongiosa in the os coxae and more in the sacrum, but overall matches well to the average female. When compared to the average male, total spongiosa volumes are much different, and there is more variation in spongiosa volume. In particular, the percentage of spongiosa in the ribs and scapulae vary greatly. One would expect differences though, due to natural skeletal variation.

A comparison of spongiosa volume and percentage of total for reference female and reference male (RM) was made. Although the spongiosa varied, as expected due to patient size, the

percentage of spongiosa volume for both reference individuals was comparable. A higher percentage of spongiosa volume was seen in the os coxae of RF compared to RM, and lower percentages of spongiosa volume in the femora and humeri.

#### 4.2. Marrow Volume Fraction Averages

Marrow Volume Fractions (MVF) were obtained for the 13 skeletal sites containing active marrow through the microCT imaging techniques described above. Since multiple cuboidal samples were taken from several sites, MVF's had to be averaged to give a mass estimate by skeletal site. If the volume of the separate sites was known (as in left and right sites), then the MVF was volume weighted between the two sides. If volumes weren't known (as in the ilium, pubis, and ischium of the os coxae) a straight average of the three sites was performed. The same method was used to average Endosteum Volume Fractions (EVF). A more detailed definition of MVF and EVF averaging for all skeletal sites is given in Appendix A and B.

It is noted that the MVF are similar for a single bone site except in the cranium and femora. The cranium has MVF variation from 11% marrow in the occipital lobe to about 39% - 43% marrow in the frontal and occipital lobes. The femoral neck is 87% marrow, whereas the femoral head is 71% marrow. An image of the microstructure of the frontal lobe and femoral head are given in Fig 7 and 8, respectively. . Since the microstructure varied greatly in these skeletal sites, volume averaging seemed best.

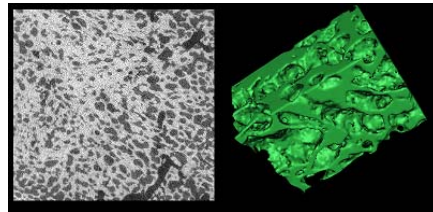


**Figure 7. Microstructure of the frontal lobe (40% marrow).**

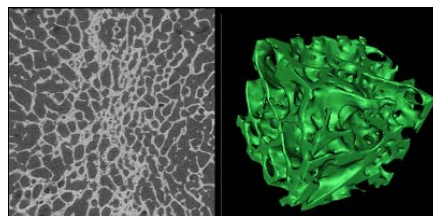


**Figure 8 Microstructures of the femoral head (71% marrow).**

#### 4.3 Mass Calculations

Masses for the trabecular spongiosa region and cortical bone regions for the skeletal sites containing active marrow, and those not containing active marrow are given in Table I and II, respectively. The percent active marrow for the os coxae, ribs and cranium was found to differ greatly from those values given in ICRP 70/89 reference man. Both the cranium and rib estimates were much higher compared to RF, and the os coxae was much lower. It is

emphasized again that the mass of RF is not bound by cellularity, and is given at ICRP 70/89 reference values only for comparison.

Since no ICRP female model exists, data contained in a study at the University of Florida on the derivation of skeletal masses in the current ICRP age series was used to compare UF RF to a reasonable ICRP female. That ICRP skeletal study served to provide a skeletal site specific estimate of the masses of a 40 year old female from the ICRP 70/89 reference man data. The data given should be the best estimate of female skeletal masses, as recommended by the ICRP and serves as a fair comparison of UF RM to any sort of reference model available.

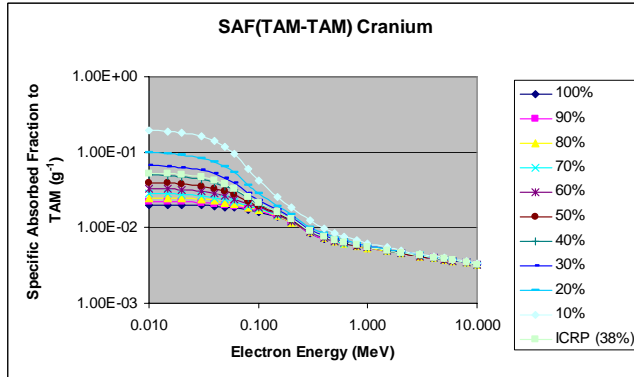
A final comparison is made between the ICRP 70/89 35 year old female recommendations and the UF reference female model in Table III. By definition the total skeleton is the sum of the bone, active marrow, inactive marrow, cartilage, and miscellaneous which does not include periarticular tissue or blood. Large differences in active marrow, inactive marrow, bone and total skeletal masses are seen. Possible reasons for differences include the ICRP definition of reference female not including masses of a real person, but instead are guesses at what the correct mass should be. Also, masses and other data used come from studies dated back to as far as 1926. The methods used in the mass calculation of UF RF use the most recent advances in both technology and the literature.

#### **4.4 Absorbed Fraction Data**

##### **4.4.1 Bone site Specific Absorbed Fractions**

SAF's for each individual bone site was tabulated for two targets – Trabecular Active Marrow (TAM) and Shallow Trabecular Active Marrow (TAMs) and all five sources. A TAMs target followed the same trends as TAM as a target, but with slightly lower SAF's. The SAF(TAM-TAM) decreased with higher energy since higher energy particles will have enough energy to escape the TAM and deposit energy elsewhere. At low energies and at high cellularity (no fatty marrow), the absorbed fraction is at a maximum because all of the particles are absorbed in the active marrow. Conversely, at low energies and low cellularity (fatty marrow), the particles are absorbed in the fat and there is a low absorbed fraction to the TAM. Calculating the SAF causes a division of the mass of the target which depends on the cellularity, thus, cellularity trends are switched. There is a point of convergence where cellularity no longer matters at an intermediate energy. This is shown in Fig 7.

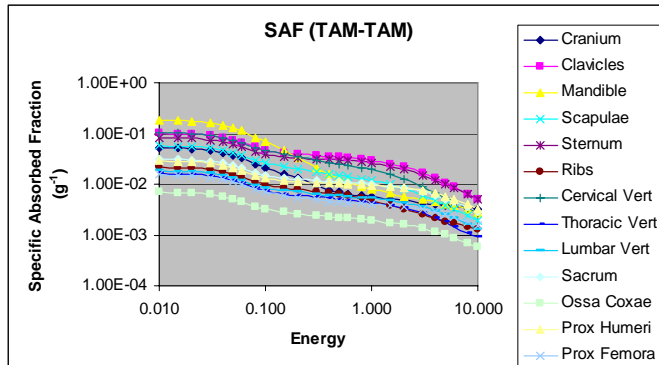
**Figure 7. Specific Absorbed Fraction for Trabecular Active Marrow (TAM) source irradiating a TAM target in the cranium.**



**4.4.2 Specific Absorbed Fractions for all bone sites**

SAF’s were tabulated for two targets – TAM and TAMs and all five sources for all bone sites together. The TAMs target followed the same trends as the TAM target but with lower values. At low energies, the SAF(TAM-TAM) was highest for those bone sites with small marrow cavities (e.g. mandible, cervical vertebrae, sternum, cranium). At higher energies, the same trend was followed except for the mandible. The SAF(TAM-TAM) is decreasing over energy because at higher energies more particles leave the marrow regions. The bone site with the lowest SAF(TAM-TAM) was the ossa coxae, where there is a large amount of active marrow and large cavities, as shown in Fig 8.

**Figure 8. Specific Absorbed Fraction for Trabecular Active Marrow (TAM) source irradiating a TAM target in all bone sites.**



**4.4.3 Specific Absorbed Fractions for all sources**

SAF’s were graphed for two targets – TAM and TAMs and all five sources for each bone site. All sources followed the same trends for each bone site. The SAF(TAM-TAM) had the highest value and decreased slightly with increasing energy. The SAF(TAM-TBS) followed the same trend as an active marrow source, but was slightly lower in value. This is because there would be less energy deposited in the active marrow for a particle starting in the trabecular bone surface

than there would be for actually starting in the active marrow. The SAF(TAM-TIM) slightly increases with increasing energy and levels off to the same value as active marrow and trabecular bone surface values. A particle would need to have enough energy to leave the inactive marrow in order to deposit energy into the active marrow regions. The SAF(TAM-TBV) is the second lowest value and follows the same trend as an inactive marrow source. The lowest SAF is found for a cortical bone volume source where the SAF(TAM-CBV) increases with increasing energy and then decreases at very high energies. This is because a particle needs to have a significant amount of energy to leave the cortical bone volume and deposit energy into the active marrow. At very high energies, the particle leaves the active marrow. An example of the cranium is shown in Fig 9.

**Figure 9. Specific Absorbed Fraction for all sources irradiating the Trabecular Active Marrow (TAM) in the cranium.**

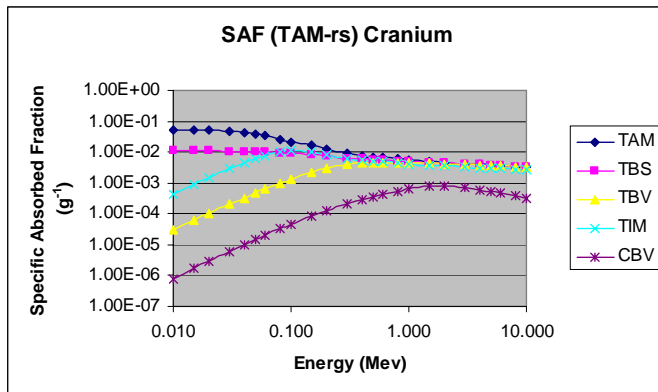


**Table I. Reference female masses for the trabecular spongiosa and cortical bone regions for the skeletal sites containing active marrow.**

Skeletal Site (w/active marrow)	Trabecular Spongiosa Regions				Cortical Bone Regions		
	Spongiosa	Marrow	Endosteum	Trabecular Bone	Trabecular Bone	Cortical	Cortical Bone
	Volume (cm <sup>3</sup> )	Volume Fraction	Volume Fraction	Volume Fraction	Mass (g)	Volume (cm <sup>3</sup> )	Mass (g)
<b>Os Coxae</b>	407.65	0.87	0.06	0.13	98.70	212.99	408.93
<b>Cervical Vertebrae</b>	31.67	0.78	0.10	0.22	13.19	4.88	9.36
<b>Thoracic Vertebrae</b>	171.51	0.90	0.06	0.10	32.73	6.65	12.76
<b>Lumbar Vertebrae</b>	151.47	0.91	0.05	0.09	27.48	13.60	26.11
<b>Sacrum</b>	83.25	0.96	0.02	0.04	5.63	40.84	78.41
<b>Clavicles</b>	25.94	0.96	0.02	0.04	2.02	9.99	19.17
<b>Right</b>	13.63	0.96	0.02	0.04	1.00	10.01	19.22
<b>Left</b>	12.32	0.96	0.02	0.04	1.02	9.96	19.13
<b>Femora, proximal</b>	205.94	0.81	0.08	0.19	75.72	33.33	63.99
<b>Right</b>	257.82	0.81	0.08	0.19	95.88	33.93	65.15
<b>Left</b>	152.06	0.81	0.08	0.19	55.21	32.69	62.77
<b>Humerii, proximal</b>	105.76	0.95	0.03	0.05	10.05	20.63	39.60
<b>Right</b>	*	*	*	*	*	*	*
<b>Left</b>	46.30	0.95	0.03	0.05	4.40	10.31	19.80
<b>Scapulae</b>	56.73	0.77	0.09	0.23	24.53	27.52	52.85
<b>Right</b>	28.48	0.87	0.06	0.13	6.95	28.27	54.28
<b>Left</b>	28.25	0.68	0.01	0.32	17.57	26.78	51.42
<b>Sternum</b>	30.59	0.99	0.01	0.01	0.73	16.23	31.16
<b>Mandible</b>	15.42	0.89	0.06	0.11	3.28	22.07	42.38
<b>Ribs TOTAL</b>	128.42	0.93	0.04	0.07	17.06	180.81	347.15
<b>Cranium</b>	133.59	0.33	0.14	0.67	171.34	261.36	501.81
<b>Facial bones</b>	1.86	0.89	0.06	0.11	0.40	24.90	47.80

**Table II. Reference female masses for the trabecular spongiosa and cortical bone regions for the skeletal sites without active marrow.**

Skeletal Site	Trabecular Spongiosa Regions				Cortical Bone Regions		
	Spongiosa	Marrow	Endosteum	Trabecular Bone	Trabecular Bone	Cortical	Cortical Bone
	w/o active marrow Volume (cm <sup>3</sup> )	Volume Fraction	Volume Fraction	Volume Fraction	Mass (g)	Volume (cm <sup>3</sup> )	Mass (g)
<b>Femora</b>	340.93				75.83	254.28	488.22
<b>medullary cavity</b>	42.84	*	0.01	*	*	140.11	269.01
<b>distal end</b>	298.09	0.87	0.07	0.13	75.83	114.17	219.20
<b>Fibula</b>	45.15				7.15	57.76	110.91
<b>proximal</b>	14.76	0.87	0.07	0.13	3.76	8.00	15.37
<b>medullary cavity</b>	17.05	*	0.02	*	*	37.29	71.60
<b>distal</b>	13.34	0.87	0.07	0.13	3.39	12.47	23.94
<b>Tibia</b>	343.77				82.80	210.06	403.31
<b>proximal</b>	238.62	0.87	0.07	0.13	60.71	98.80	189.69
<b>medullary cavity</b>	18.31	*	0.01	*	*	56.37	108.22
<b>distal</b>	86.84	0.87	0.07	0.13	22.09	54.89	105.39
<b>Humerii</b>	53.56				2.55	36.59	70.25
<b>medullary cavity</b>	26.73	*	0.01	*	*	22.88	43.93
<b>distal end</b>	26.83	0.95	0.03	0.05	2.55	13.71	26.32
<b>Ulna</b>	19.30				1.28	38.27	73.48
<b>proximal</b>	10.46	0.95	0.03	0.05	0.99	12.66	24.32
<b>medullary cavity</b>	5.87	*	0.02	*	*	20.29	38.96
<b>distal</b>	2.97	0.95	0.03	0.05	0.28	5.31	10.20
<b>Radius</b>	27.27				2.21	44.17	84.81
<b>proximal</b>	8.42	0.95	0.03	0.05	0.80	9.29	17.84
<b>medullary cavity</b>	3.98	*	0.02	*	*	20.86	40.04
<b>distal</b>	14.87	0.95	0.03	0.05	1.41	14.03	26.93

**Table III. Comparison between the ICRP 70/89 35 year old female skeletal mass recommendations and the UF reference female model.**

Subject Parameter	ICRP 70 35 y female	UF Reference Female	Difference
	Mass (g)	Mass (g)	%
height (cm)	163	160	
weight (kg)	60	61	
BMI kg/m <sup>2</sup>	22.58	23.83	
Age	35	64	
Total Skeleton	7800	6592.11	18.32%
Bone	4000	3462.34	15.53%
Active Marrow	900	687.29	30.95%
Inactive marrow	1800	1342.48	34.08%
Cartilage	900	900	
Miscellaneous	200	200	

## 5. CONCLUSION

A complete skeletal mass and absorbed fraction database has been given for a reference female model to be used to provide a patient specific scalable model for accurate dose assessment in radiation protection and medical applications. No model for a female subject has previously been given, and this paper serves to provide a companion skeletal reference model to the adult male. It is hoped that this model will be used to better assess dose estimates of the female population.

## ACKNOWLEDGMENTS

I would like to express my gratitude first and foremost to Dr. Wesley Bolch for his guidance through the work of this master's project. His leadership and personal care for both his students and the publications of the Bone Imaging Dosimetry group is unprecedented. I would like to thank the United States Department of Energy for funding me under the Health Physics Fellowship. Also, I am thankful for the time, effort, and help of the previous students in the group - Jim Brindle, Amish Shah, and Didier Rajon. I am also much obliged to my family for their support and my friends for their patience.

## REFERENCES

1. Bolch WE, Patton PW, Shah AP, and Rajon DA 2002b “Considerations of anthropomorphic, tissue volume, and tissue mass scaling for improved patient specificity of skeletal S values.” *Med Phys* **29(6)** 1054-1070.
2. Brindle J “Techniques for Skeletal Dosimetry in Radionuclide Therapy via Assessment of Patient Specific Total and Regional Spongiosa Volumes” [*Dissertation*]. Gainesville, FL: University of Florida. **300**; 2006.
3. ICRP 1975 “Report on the Task Group on Reference Man.” Oxford, UK: *International Commission of Radiological Protection*. **ICRP Publication 23**.
4. ICRP 1995 “Basic anatomical and physiological data for use in radiological protection: the skeleton.” Oxford, UK: *International Commission of Radiological Protection*. **ICRP Publication 70**.
5. ICRP 2002 “Basic anatomical and physiological data for use in radiological protection: reference values.” New York, New York: *International Commission of Radiological Protection*. **ICRP Publication 89**.
6. Marieb EN 2005 “Human anatomy and physiology, 5<sup>th</sup> edition.” Benjamin-Cummings Science Publishing, Menlo Park, CA, 2001.
7. Shah AP “Reference skeletal dosimetry model for an adult male radionuclide therapy patient based on 3d imaging and paired-image radiation transport.” [*Dissertation*]. Gainesville, FL: University of Florida. **491** p; 2004.
8. Rajon DA, Pichardo JC, Brindle JM, Kielar KN, Jokisch DW, Patton PW, and Bolch WE 2006 “Image Segmentation of Trabecular Spongiosa by Visual Inspection of the Gradient Magnitude”. *Phys Med Biol* (in press).
9. Watchman CJ, Bolch, WE 2006 “Derivations of Skeletal Masses in the Current ICRP Age Series: Considerations of a 10- $\mu$ m and 50- $\mu$ m Endosteum.” *Phys Med Biol* (in press).
10. Yao WJ, Wu CH, Wang ST, Chang CJ, Chiu NT, and Yu CY 2000 “Differential Changes in Bone Mineral Density in Health Chinese: Age Related and Sex Dependent”. *Calcified Tissue International* **68** 330-336.

## APPENDIX A

Bolch WE 2006 “Reference Guide for Image-Based Skeletal Tissue Masses”. Gainesville, FL: University of Florida. (available upon request).

## APPENDIX B

Kielar KN, Shah AP, Bolch WE 2007 “A Skeletal Reference Dosimetry Model for the Adult Female”. Gainesville, FL: University of Florida. (full paper available upon request).